Robotica (2016) volume 34, pp. 1227–1242. © Cambridge University Press 2014
doi:10.1017/S0263574714002215

Balance control of planar biped robots using virtual holonomic constraints

Yong Hu†* and Zhiyun Lin‡

†*Science and Technology on Space Intelligent Control Laboratory, Beijing Institute of Control Engineering, Beijing 100190 P. R. China*
‡*The State Key Laboratory of Industrial Control Technology and College of Electrical Engineering, Zhejiang University, Hangzhou 310027 P. R. China, and the School of Electrical Engineering and Computer Science, University of Newcastle, Callaghan, NSW 2308, Australia*
Email: linz@zju.edu.cn

(Accepted July 22, 2014. First published online: August 15, 2014)

SUMMARY
The balance control problem of planar bipedal robots during disturbed standing is investigated. Virtual holonomic constraints which specify the angles of actuated joints as a function of the rotation angle between the sole of the stance foot and the ground are recalled. These constraints enable the robot to avoid turnover during external disturbances similar to how a human being would react. Moreover, for a disturbance beyond the balance conditions for single-leg support, the robot changes to a double support posture to avoid turnover by the virtual holonomic constraints. Further, for a special kind of balance: standing on toe which leads to underactuation, we also give the design conditions of the virtual holonomic constraints.

KEYWORDS: Biped robot; Stable standing; Underactuated system.

1. Introduction

This paper investigates the problem of balance control for planar biped robots. Balance control is essential for biped robots in achieving dynamic walking. The Zero Moment Point (ZMP) based approach is one major method for balance control.[1] For this method, foot rotation is not allowed to occur.[2–5] That is, the ZMP remains inside the convex hull of the foot support region to ensure the upright posture in standing or walking. Moreover, by regulating the ZMP, the landing location of the stepping foot can be controlled to realize a stable walking.[6] However, it is usually energy-costly and the walking gait looks unnatural for bipedal robots with the ZMP based control.

To achieve high-efficient walking or a more natural walking gait, relaxing the ZMP constraint is a key factor. In ref. [7], foot rotation is considered by directly regulating the ZMP and the existence and uniqueness condition of a periodic motion including the foot rotation subphase is presented. Similarly, the authors of[8] adopt the same idea for jumping control of a planar biped. Moreover, human-like 3D walking is investigated in ref. [9] by taking into account foot rotation with the objective of minmizing the torque input. In short, as shown in these works, a foot rotation subphase in each walking step is helpful in reducing the energy cost.

On the aspect of stable standing subject to external disturbances, a passivity based approach is proposed in ref. [10], which takes the similar idea as for stable walking control using the ZMP information and does not include a foot rotation subphase. However, for a large disturbance, foot rotation may be an effective strategy in responding to the disturbance similar to how a human being would react. To our best knowledge, such an idea has not been explored yet for stable standing.

In this paper, the balance control problem of a planar biped robot is investigated by taking into consideration of a human-like foot rotation subphase in responding to large external disturbances. Inspired by many works that use virtual holonomic constraints for the study of underactuated

* Corresponding author. E-mail: nhhy@hotmail.com

https://doi.org/10.1017/S0263574714002215 Published online by Cambridge University Press

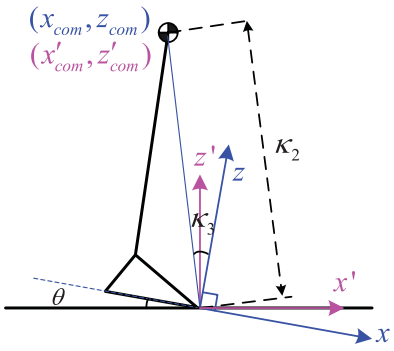


Fig. 1. A simplified biped robot having foot turnover.

Euler-Lagrange systems[11] such as Pendubot,[12] bicycles,[13] and biped robots,[14–16] we also adopt the idea of using virtual holonomic constraints for the purpose of designing a stable standing control law. With this method, we can explicitly design a complete motion integrating the subphase of foot toe support and moreover, the closed-loop dynamics can be reduced to a second-order system, called the zero dynamics. Then by investigating the zero dynamics, sufficient conditions are obtained to avoid turnover. In particular, when the disturbances are small, the standing posture is stabilized with a single foot support allowing to have foot rotation. Moreover, when the disturbances are too large, then the robot switches to the double foot support posture to avoid turnover. The critical condition for switching between the two support postures is also provided. The advantages of our approach are as follows. First, the robot under the proposed control can resist large external disturbances. Second, the region ensuring non-turnover can be obtained analytically. Finally, the idea developed in this paper can also be generalized to achieve more complex human-like behaviors on robots such as performing pirouette.

2. Robot Model

2.1. Swing phase

In this paper, we consider a planar biped with several rigid links connected by idea joints. Each joint is assumed to be independently actuated. The main problem considered in this paper is the balance control problem with single foot support. It is certain that if there are no disturbances, the robot keeps a fixed posture in single support on a flat foot. When the stance heel rises from the ground subject to external disturbances, then the robot begins to roll over the stance toe and becomes underactuated. In this case, the stance toe is assumed to act as a pivot.

Our aim is to maintain the angle between the stance foot and the ground, i.e., θ in Fig. 1, in a specific range. Let n be the number of joints. We define the $(n+1)$-dimensional generalized coordinates as $q = [\theta, q_1, q_2, \ldots, q_n]^T$. Considering the Lagrange's formula

$$\frac{d}{dt}\frac{\partial L}{\partial \dot{q}} - \frac{\partial L}{\partial q} = Bu,$$

we obtain the equation of motion

$$D(q_a)\ddot{q} + C(q, \dot{q})\dot{q} + G(q) = Bu, \tag{1}$$

where $q_a = [q_1, q_2, \ldots, q_n]^T$ is the generalized coordinates of actuated joints, $D(q) \in \mathbb{R}^{(n+1)\times(n+1)}$ is the inertia matrix, $C(q, \dot{q}) \in \mathbb{R}^{(n+1)\times(n+1)}$ is the matrix of Coriolis and centrifugal terms, $G(q) = \frac{\partial V}{\partial q} \in \mathbb{R}^{(n+1)\times 1}$ is the gradient of the potential energy, $u = [u_1, u_2, \ldots, u_n]^T$ is the vector of torques applied to the joints, and $B \in \mathbb{R}^{(n+1)\times n}$ describes the effects of actuators on the generalized coordinates.

https://doi.org/10.1017/S0263574714002215 Published online by Cambridge University Press

2.2. Impact model

The evolution of Lagrangian dynamics is discontinuous at the instants when the sole of the stance foot touches the ground. Touchdown impact results in an instantaneous change of the velocities of the generalized coordinates, but the generalized coordinates remain continuous. That is,

$$D(q_a)(\dot{q}^+ - \dot{q}^-) = J^T \lambda. \tag{2}$$

The superscripts - and + denote the state value before and after the instantaneous impacts, respectively, λ is the torque impulse that occurs at touchdown impact, $J = [1, 0_{1\times n}]$ is obtained from the constraint $\dot{\theta}^+ = 0$ after the impact since the stance foot acts as an ideal pivot without rebound and slipping, and

$$J\dot{q}^+ = 0. \tag{3}$$

From (2), we have

$$\dot{q}^+ = \dot{q}^- + D^{-1}J^T\lambda. \tag{4}$$

From (3) and (4), we obtain the torque impulse

$$\lambda = -(JD^{-1}J^T)^{-1}J\dot{q}^-. \tag{5}$$

Substituting (5) into (4) leads to the following impact model:

$$\dot{q}^+ = \Delta(q_a)\dot{q}^-, \tag{6}$$

where $\Delta(q_a) = I - D^{-1}J^T(JD^{-1}J^T)^{-1}J$. It should be noted that the impact introduced here is caused by the rotation around the stance toe or heel while the impacts in biped walking or running[17] are caused by the translations of swing foot. The impact models are totally different.

3. Virtual Holonomic Constraints and Zero Dynamics

Virtual holonomic constraints are used to synchronize the evolution of the robot's joints throughout a stride in order to achieve a gait.[17] The constraints are virtual because they arise due to the actions of feedback control rather than some physical configurations.

Inspired by this method, we employ virtual constraints to synchronize the evolution of the actuated joints and put up with the rotation around the stance toe or heel.

The virtual constraints are parametrized by θ and can be expressed in the form

$$y = h(q) = q_a - h_d(\theta) \tag{7}$$

where $q_a = (q_1, q_2, \ldots, q_n)$ is the vector of actuated coordinates and $h_d(\cdot)$ is a function constructed based on *Bézier* polynomials.[18]

The feedback control law

$$u^* = \left(\frac{\partial h(q)}{\partial q}D^{-1}(q_a)B\right)^{-1}\left(\frac{\partial^2 h_d(\theta)}{\partial\theta^2}\dot{\theta}^2 + \frac{\partial h(q)}{\partial q}D^{-1}(q_a)(C\dot{q} + G)\right)$$

ensures the virtual constraint $y = q_a - h_d(\theta) = 0$ when initially the constraint is satisfied. Moreover, in order to make the system asymptotically stable, the following control law is proposed:[17]

$$u = u_0(q, \dot{q}) = u^* - \left(\frac{\partial h(q)}{\partial q}D^{-1}(q_a)B\right)^{-1}(K_d\dot{y} + K_p y), \tag{8}$$

where the parameters K_d and K_p are chosen such that

$$\ddot{y} + K_d\dot{y} + K_p y = 0 \tag{9}$$

https://doi.org/10.1017/S0263574714002215 Published online by Cambridge University Press

is asymptotically stable. Then, there exists a smooth zero dynamics manifold[14,19] with the output function (7), that is,

$$\mathcal{Z} = \{[q, \dot{q}]^T | h(q) = 0, \frac{\partial h}{\partial q}\dot{q} = 0\}. \tag{10}$$

The zero dynamics in terms of $[\theta, \sigma]^T = [\theta, D_1(q)\dot{q}]^T$ can be written as

$$\begin{aligned} \dot{\theta} &= \kappa_1 \sigma \\ \dot{\sigma} &= -G_1([\theta, h_d(\theta)]^T) \end{aligned} \tag{11}$$

where $\kappa_1 = \frac{1}{D_1([\theta, h_d(\theta)]^T)[1, \frac{\partial h_d}{\partial \theta}]^T}$, and D_1 and G_1 are the first rows of D and G, respectively. Moreover, it is known that

$$G_1([\theta, h_d(\theta)]^T) = mgx'_{com}(\theta),$$

where x'_{com} is the distance between the stance toe and the projection point of the center of mass (COM) in the horizontal plane which is shown in Fig. 1 and

$$x'_{com}(\theta) = -\kappa_2 \sin(\theta - \kappa_3),$$

where

$$\begin{aligned} \kappa_2 &= \sqrt{x^2_{com}(h_d(\theta)) + z^2_{com}(h_d(\theta))}, \\ \kappa_3 &= -\tan^{-1}(\frac{x_{com}(h_d(\theta))}{z_{com}(h_d(\theta))}), \end{aligned}$$

and (x_{com}, z_{com}) is the position of the COM in $x - z$ coordinate system which is shown in Fig. 1.

The zero dynamics can be rewritten as[17]

$$\begin{aligned} \dot{\theta} &= \kappa_1 \sigma, \\ \dot{\sigma} &= mg\kappa_2 \sin(\theta - \kappa_3), \end{aligned} \tag{12}$$

where κ_1, κ_2, and κ_3 are functions of θ.

Let us introduce some assumptions useful to obtain the results of this paper.

Assumption A.1 For single support, the stance foot impact occurs only at the instant t at which $\theta(t) = 0$ and $\dot{\theta}(t^-) < 0$.

Assumption A.2 Foot impacts are perfectly inelastic and no bounce occurs.

The superscripts - and + denote the state value before and after instantaneous impacts, respectively. We design the virtual holonomic constraints $h_d(\theta)$ for stable standing such that the following conditions hold.

Condition C.1

$$\frac{\partial h_d}{\partial \theta}|_{\theta=0} = 0.$$

Condition C.2 $x_{com}(h_d(0))$ is in the convex hull of the foot support region.

Condition C.1 means that if the stance foot stops rotating relative to the ground, the actuated joints will also stop. **Condition C.2** means that when the robot restores to the single support posture on a flat foot (i.e., $\theta = 0$), the virtual holonomic constraints can guarantee that the robot is statically stable.

Lemma 3.1. *Suppose Assumptions A.1–A.2 and Conditions C.1–C.2 hold. Then the impact occurs at t if and only if* $\theta(t^-) = 0$ *and* $\sigma(t^-) < 0$.

https://doi.org/10.1017/S0263574714002215 Published online by Cambridge University Press

Proof. ($\Leftarrow$) When an impact occurs at t, we have $\theta(t^-) = 0$ and $\dot{\theta}(t^-) < 0$. According to Condition C.1, we get

$$\begin{aligned} \kappa_1 &= \frac{1}{D_1([\theta, h_d(\theta)]^T)[1, \frac{\partial h_d}{\partial \theta}]^T} \\ &= \frac{1}{d_{11}([0, h_d(0)]^T)} \\ &> 0 \end{aligned}$$

where d_{11} is the element of the first row and first column of D. Then, we have $\sigma(t^-) = \kappa_1 \dot{\theta}(t^-) < 0$.

($\Rightarrow$) If $\sigma(t^-) < 0$, then, $\dot{\theta}(t^-) = \kappa_1^{-1}\sigma(t^-) < 0$. Taking into account $\theta(t^-) = 0$, from Assumption A.1, we can get that an impact occurs. ■

4. Stability Analysis

4.1. Perturbed standing

First, we consider the special situation where the robot is in single support subject to a velocity perturbation. The initial values of the zero dynamics are $\theta(0) = 0$ and $\sigma(0) = \sigma_0$.

From (12), we have

$$\frac{d\sigma}{d\theta} = \frac{mg\kappa_2 \sin(\theta - \kappa_3)}{\kappa_1 \sigma}. \tag{13}$$

Then, integrating on both sides of (13) we obtain

$$\sigma_0^2 - \sigma^2 = 2V_1(\theta), \tag{14}$$

where

$$V_1(\theta) = -\int_0^\theta \frac{\kappa_2}{\kappa_1} mg \sin(\theta - \kappa_3) d\theta. \tag{15}$$

For the given virtual constraints $h_d(\theta)$, suppose that $V_1(\theta)$ reaches its maximum value at $\theta = \theta^\star$. That is,

$$V_1(\theta^\star) = \max_{0 \le \theta \le \theta_m} V_1(\theta) = V_1^{max}$$

where θ_m is the maximum value that θ can vary and V_1^{max} is the maximum value of $V_1(\theta)$. Thus, we have

$$\frac{\partial V_1(\theta)}{\partial \theta}\Big|_{\theta=\theta^\star} = \frac{\kappa_2}{\kappa_1} mg \sin(\theta - \kappa_3)|_{\theta=\theta^\star} = 0.$$

Then, $\theta = \theta^\star$, $\sigma = 0$ is an equilibrium point.

Next, we present a necessary and sufficient condition for turnover prevention when the angle between the stance foot and the ground is zero. In this paper, only the forward fall is considered as the backward fall can be treated in the same way.

Theorem 4.1. *Let $h_d(\theta)$ be the given virtual constraints, with $\theta(0) = 0$ and $\sigma(0) = \sigma_0$. No forward fall occurs before the stance foot impact if and only if*

$$\sigma_0 \le \sqrt{2V_1^{max}}$$

Proof. ($\Rightarrow$) If the forward fall does not occur, then

$$0 \le \theta \le \theta_m.$$

Note that $\theta(t)$ is differentiable and bounded when $t \in [0, T_m]$ where T_m is the moment when the impact occurs or ∞. There are two cases.

https://doi.org/10.1017/S0263574714002215 Published online by Cambridge University Press

i) For $t \in [0, T_m]$, $\theta(t)$ is monotonous. In this case, the impact will not occur because $\theta(0) = \theta(T_m) = 0$ contradicts the monotonicity of $\theta(t)$. Then, $T_m = \infty$. We assume

$$\lim_{t\to\infty} \theta(t) = \theta_{lim}$$

where θ_{lim} is a constant. Note that $\theta(t)$ is differentiable, so we have

$$\lim_{t\to\infty} \dot{\theta}(t) = 0$$

and

$$\lim_{t\to\infty} \sigma(t) = 0.$$

From (14), we have

$$\sigma_0 = \sqrt{2V_1(\theta_{lim})} \leq \sqrt{2V_1^{max}} \tag{16}$$

ii) For $t \in [0, T_m]$, $\theta(t)$ is not monotonous. Then, there exist t_1 and t_2 such that $\theta(t_1) = \theta(t_2)$. Moreover, $\theta(t)$ is continuous for $t \in [t_1, t_2]$ and differentiable for $t \in (t_1, t_2)$. By Lagrange Mean Value Theorem, there exists $t_3 \in (t_1, t_2)$ such that $\dot{\theta}(t_3) = 0$. Then, $\sigma(t_3) = 0$. From (14), we have

$$\sigma_0 = \sqrt{2V_1(\theta(t_3))} \leq \sqrt{2V_1^{max}}. \tag{17}$$

($\Leftarrow$) We consider three cases.

i) For $\sigma_0 = \sqrt{2V_1^{max}}$, if the forward fall occurs, then there exists t_1 such that $\theta(t_1) = \theta^\star$ and $V_1(\theta(t_1)) = V_1^{max}$. Considering (14), we have $\sigma(t_1) = 0$. Since $\theta = \theta^\star, \sigma = 0$ is an equilibrium point, the states of the system will remain constant, a contradiction. Thus, we know that no forward fall occurs.

ii) If $0 \leq \sigma_0 < \sqrt{2V_1^{max}}$, then it follows from (14) that

$$\max_{0\leq t\leq\infty} V_1(\theta(t)) \leq \frac{1}{2}\sigma_0^2 < V_1^{max}, \tag{18}$$

which means $\theta \neq \theta^\star$ for $t \in [0, \infty)$. Since $\theta(t)$ is continuous and $\theta(0) = 0$, we can get $\theta < \theta^\star$ for $t \in [0, \infty)$.

iii) If $\sigma_0 < 0$, then $\dot{\theta}_0 < 0$. Since $\theta_0 = 0$, according to Lemma 3.1, we can know the impact occurs. Thus, no forward fall occurs before the impact. ■

Next, we analyse the conditions such that the stance foot rotation does not occur after the impact.

According to Lemma 3.1, when an impact occurs, $\theta = 0$ and $\sigma^- < 0$. Considering (14), we obtain that $\sigma^- = -|\sigma_0|$. Then, we get $\dot{\theta}^- = -\frac{|\sigma_0|}{\kappa_1}$.

By the impact model (6) and Condition C.1, the angle velocities $\dot{q}_a^+$ just after the impact can be derived as

$$\dot{q}^+ = \begin{bmatrix} 0 \\ \dot{q}_a^+ \end{bmatrix} = \Delta(q_a)\dot{q}^- = \Delta(q_a)\begin{bmatrix} 1 \\ 0 \end{bmatrix}\dot{\theta}^-. \tag{19}$$

Denote $\Phi(t) = \exp([\begin{smallmatrix} 0_{6\times6} & I_{6\times6} \\ -K_p & -K_d \end{smallmatrix}]t)$. Then, from the moment just after the impact, the solution of (9) can be equivalently represented as

$$\begin{bmatrix} q_a(t) \\ \dot{q}_a(t) \end{bmatrix} = \begin{bmatrix} h_d(0) \\ 0_{6\times1} \end{bmatrix} + \Phi(t)\begin{bmatrix} 0_{6\times1} \\ \dot{q}_a^+ \end{bmatrix}. \tag{20}$$

According to (1), we get $\ddot{q}_a(t)$ immediately. Then, using the Newton-Euler equations, we can get the function of the ground reaction force F_x, F_z, and the position of ZMP x_{ZMP}. It should be emphasized that, when the virtual constraints $h_d(\theta)$ are given, the system evolution after the impact only depends on σ_0. Then, we can find the minimum value σ_0^m such that the ZMP constraint, unilateral

https://doi.org/10.1017/S0263574714002215 Published online by Cambridge University Press

constraint, and friction constraint are satisfied. Because the ground reaction force and system state are all explicit functions of time, the calculations of σ_0^m are easy to perform. Then, we reach the conclusion that the condition to avoid stance foot rotation after the impact is $\sigma_0 \geq \sigma_0^m$.

Next, we analyse a more general case based on Theorem 4.1. The robot is in single support and is subject to both velocity and angle perturbations. The initial values of the zero dynamics are $\theta(0) = \theta_0 > 0$ and $\sigma(0) = \sigma_0$.

Theorem 4.2. *Let $h_d(\theta)$ be the given virtual constraints, $\theta^\star > \theta(0) = \theta_0 > 0$ and $\sigma(0) = \sigma_0$. No forward fall occurs before the stance foot impact if*

$$|\sigma_0| < \sqrt{2V_{\theta_0}^{max}} \tag{21}$$

where

$$V_{\theta_0}^{max} = V_1^{max} - V_1(\theta_0).$$

Proof. Integrating (13) from θ_0 to θ results in

$$\frac{1}{2}\sigma_0^2 - \frac{1}{2}\sigma^2 = V_1(\theta) - V_1(\theta_0). \tag{22}$$

Considering (21), we obtain

$$\frac{1}{2}\sigma(\theta) + V_1(\theta) < V_1^{max}. \tag{23}$$

Notice that θ is continuous and $\theta_0 < \theta^\star$. Moreover, when $\theta = \theta^\star$, (23) does not hold. Hence, we can get that $\theta < \theta^\star$ and no forward fall occurs before the stance foot impact. ■

Remark 4.1. *Theorem 4.1 and Theorem 4.2 give the ranges of θ_0 and σ_0 to prevent forward fall of the robot under the assumption that several necessary constraints such as the ZMP constraint, unilateral constraint, actuator saturation constraint, and friction constraint are satisfied. In practice, we should calculate the ground reaction force F_x, F_z, the actuator output, and the position of ZMP x_{ZMP} from the Newton-Euler equations and system dynamics in order to check these necessary constraints. Then, the ranges of θ_0 or σ_0 will be further restricted.*

4.2. Single toe standing

In this subsection, we develop a condition for single toe standing, which is similar to a pirouette performed by a ballerina.[20] The difficulty is that, when standing on a toe, the robot can not directly maintain its upright posture. That is, the system is underactuated. In this subsection, we give some results about this problem.

Theorem 4.3. *Let $h_d(\theta)$ be the given virtual constraints, and let $\theta(0) = \theta_0 \in [\theta_1, \theta_2]$, $\sigma(0) = \sigma_0$. Then $\forall t > 0$, $\theta(t) \in [\theta_1, \theta_2]$ holds, if*

$$\frac{1}{2}\sigma_0^2 + V_1(\theta_0) < \min(V_1(\theta_1), V_1(\theta_2)). \tag{24}$$

Proof. We integrate (13) from θ_0 to θ, and then obtain

$$\frac{1}{2}\sigma_0^2 - \frac{1}{2}\sigma^2 = V_1(\theta) - V_1(\theta_0). \tag{25}$$

Combining (24) and (25), we obtain

$$\frac{1}{2}\sigma^2 + V_1(\theta) < \min(V_1(\theta_1), V_1(\theta_2)). \tag{26}$$

https://doi.org/10.1017/S0263574714002215 Published online by Cambridge University Press

Notice that $\theta(0) = \theta_0 \in [\theta_1, \theta_2]$ and $\theta(t)$ is continuous. Moreover, when $\theta = \theta_1$ or $\theta = \theta_2$, (26) does not hold. Thus, it is known that $\forall t > 0$, $\theta(t) \in [\theta_1, \theta_2]$. ■

For a more realistic situation, the stance toe acts as a pivot with viscous friction. Then, the zero dynamics becomes

$$\begin{aligned} \dot{\theta} &= \kappa_1 \sigma, \\ \dot{\sigma} &= mg\kappa_2 \sin(\theta - \kappa_3) - k_v \dot{\theta}, \end{aligned} \tag{27}$$

where $k_v > 0$ is the viscous friction coefficient.

Theorem 4.4. *For system* (27)*, let $h_d(\theta)$ be the given virtual constraints and let θ_1, θ_2 and θ^* be the given angles such that $\theta_1 < \theta^* < \theta_2$. If the following conditions are satisfied for $\theta \in [\theta_1, \theta_2]$:*

1) $\kappa_1 > 0$,
2) *θ^* is the unique stationary point of $V_1(\theta)$*,
3) $V_1(\theta^*) < \min(V_1(\theta_1), V_1(\theta_2))$,

then, $(\theta^*, 0)$ *is an asymptotically stable equilibrium point of system* (27) *and the set*

$$\begin{aligned} \mathcal{B} = \quad & \{(\theta, \sigma) | \tfrac{1}{2}\sigma^2 + V_1(\theta) \leq \min(V_1(\theta_1), V_1(\theta_2)), \\ & \theta \in [\theta_1, \theta_2]\}. \end{aligned}$$

is inside its basin of attraction.

Proof. From (27), we have that

$$\sigma \frac{d\sigma}{d\theta} = \frac{mg\kappa_2 \sin(\theta - \kappa_3)}{\kappa_1} - k_v \sigma. \tag{28}$$

Then, we integrate (28) from θ^* to θ and obtain that

$$\sigma_{\theta^*}^2 - \sigma^2 = 2V_1(\theta) - 2V_1(\theta^*) + 2k_v \int_{\theta^*}^{\theta} \sigma d\theta, \tag{29}$$

where

$$V_1(\theta) = -\int_0^{\theta} \frac{\kappa_2}{\kappa_1} mg \sin(\theta - \kappa_3) d\theta. \tag{30}$$

It yields

$$\frac{\partial V_1(\theta)}{\partial \theta} = -\frac{\kappa_2}{\kappa_1} mg \sin(\theta - \kappa_3). \tag{31}$$

Since θ^* is the unique stationary point of $V_1(\theta)$ which is differentiable, then,

$$\frac{\partial V_1(\theta)}{\partial \theta}\Big|_{\theta=\theta^*} = 0,$$

and the sign of $\frac{\partial V_1(\theta)}{\partial \theta}$ for $\theta \in [\theta_1, \theta^*)$ does not change. The same is true about $\theta \in (\theta^*, \theta_2]$. From $V_1(\theta^*) < \min(V_1(\theta_1), V_1(\theta_2))$, we can obtain

$$\frac{\partial V_1(\theta)}{\partial \theta} \begin{cases} < 0, \text{for } \theta \in [\theta_1, \theta^*), \\ = 0, \text{for } \theta = \theta^*, \\ > 0, \text{for } \theta \in (\theta^*, \theta_2], \end{cases} \tag{32}$$

Then,

$$V_1(\theta^*) = \min_{\theta_1 \leq \theta \leq \theta_2} V_1(\theta).$$

https://doi.org/10.1017/S0263574714002215 Published online by Cambridge University Press

We choose

$$V_L(\theta, \sigma) = \sigma^2 + 2V_1(\theta) - 2V_1(\theta^*)$$

as a candidate Lyaponov function. We obtain $V_L(\theta, \sigma) > 0$ for any $\theta \neq \theta^*$ and $\sigma \neq 0$. According to (29), we have that

$$V_L(\theta, \sigma) = \sigma_{\theta^*}^2 - 2k_v \int_{\theta^*}^{\theta} \sigma d\theta$$

and

$$\dot{V}_L(\theta, \sigma) = -2k_v \kappa_1 \sigma^2 \leq 0.$$

We rewrite the set $\mathcal{B}$ as

$$\mathcal{B} = \{(\theta, \sigma) \big| \theta \in [\theta_1, \theta_2], V_L(\theta, \sigma) \leq c\}$$

where $c = 2\min(V_1(\theta_1), V_1(\theta_2)) - 2V_1(\theta^*)$ is a constant. Then, $\mathcal{B}$ is a positive invariant set of (27). Note that $\mathcal{B}$ is also a compact set. Let E be the set of all points in $\mathcal{B}$ where $\dot{V}_L(\theta, \sigma) = 0$. That is,

$$E = \{(\theta, \sigma) \big| \theta \in [\theta_1, \theta_2], \sigma = 0\}$$

Since $\kappa_1 > 0$ and $\kappa_2 > 0$, the largest invariant set in E only contains the point $(\theta^*, 0)$. Then, using LaSalle's invariance principal, we obtain that every solution of (27), which starts in $\mathcal{B}$ approaches the equilibrium point $(\theta^*, 0)$. ■

Remark 4.2. *Actually, conditions 2) and 3) of Theorem 4.4 guarantee that the function* $V_1(\theta)$, $\theta \in [\theta_1, \theta_2]$ *has a convex shape with the minimum value* $V_1(\theta^*)$. *In this case, the conditions 2) and 3) can be replaced by the following condition.*

$$\frac{\partial V_1(\theta)}{\partial \theta} \begin{cases} < 0, \text{ for } \theta \in [\theta_1, \theta^*), \\ = 0, \text{ for } \theta = \theta^*, \\ > 0, \text{ for } \theta \in (\theta^*, \theta_2]. \end{cases} \tag{33}$$

Since $\kappa_1, \kappa_2 > 0$, *according to* (31), *the condition* (33) *is equivalent to*

$$\begin{cases} \theta > \kappa_3, \text{ for } \theta \in [\theta_1, \theta^*), \\ \theta = \kappa_3, \text{ for } \theta = \theta^*, \\ \theta < \kappa_3, \text{ for } \theta \in (\theta^*, \theta_2], \end{cases} \tag{34}$$

which can be directly used to design the virtual constraints.

5. Application and Simulation

In this section, two simulations are executed to validate the proposed method. We consider a planar biped robot with feet shown in Fig. 2, which has one degree of underactuation. The similar planar bipeds are studied in refs. [7, 10] for walking or balance control. Table I lists the values of the parameters used in the simulations.

5.1. Simulation for perturbed standing

We freely choose a standing posture with $q = q_s$, and $q_s = [0^\circ, 10^\circ, -20^\circ, 10^\circ, -40^\circ, 70^\circ, -10^\circ]^T$, for which the COM is inside the polygon of the stance foot. We carry out a simulation for perturbed standing in single foot support. We also consider a double stance posture in order to prevent from falling when the disturbance is large enough. The double stance posture is achieved when $\theta = \theta_m = 29.0167^\circ$. There are many methods to design virtual holonomic constraints, for example, energy optimization. In this paper, we design virtual holonomic constraints $h_d(\theta)$ by $B\acute{e}zier$ polynomials of degree 6.

https://doi.org/10.1017/S0263574714002215 Published online by Cambridge University Press

Table I. Parameters of the robot.

	Torso	Femur	Tibia	Foot
Mass(kg)	24	6.8	3.2	0.8
Size(m)	0.6	0.4	0.4	Front 0.2 Rear 0.08 Height 0.1
Inertia(kgm^2)	1.8	0.47	0.2	0.05

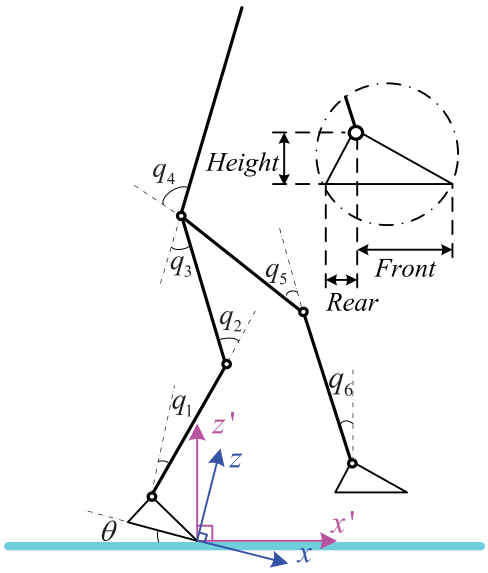


Fig. 2. Mathematical model of a planar biped robot with feet.

Through numerical calculations, the value of $V_1(\theta)$ with respect to $\theta \in [0, \theta_m]$ is drawn in Fig. 3. From the figure, we can see that when $\theta = 9.6916^\circ$, $V_1(\theta)$ reaches the maximum value V_1^{max}. By Theorem 4.1, no forward fall occurs if $\sigma_0 \leq \sqrt{2V_1^{max}} = 1368.2kg \cdot m^2\ ^\circ/s$. This corresponds to $\dot{\theta} = 29.6381^\circ/s$. Also, we can calculate the $\sigma_0 > \sigma_0^m = -5267.3kg \cdot m^2\ ^\circ/s$ to avoid stance foot rotation after the impact and the corresponding $\dot{\theta} = -114.1^\circ/s$.

Then, if $-114.1^\circ/s \leq \dot{\theta} \leq 29.6381^\circ/s$, the robot does not fall forward and the standing posture q_s can be stabilized. If $29.6381^\circ/s \leq \dot{\theta} \leq \dot{\theta}_f$, the robot switches to the double stance posture, for which $\dot{\theta}_f$ is the maximum value no forward fall can occur in the double stance posture.

First, we give a simulation with initial conditions $q(0) = q_s$, $\dot{\theta}(0) = 29^\circ/s$ and $\frac{\partial h_d}{\partial \theta}\big|_{\theta=0} = 0$. Based on the above analysis, we know the posture of standing q_s will be achieved at last. The diagrams of the resulting motion are demonstrated in Fig. 4.

In order to show that stance foot rotation does not happen after the impact, the simulated responses of the ground reaction force F_x, F_z(N), $\frac{F_x}{F_z}$, and the position of ZMP x_{ZMP}(m) after the impact are shown in Fig. 5. From the figure, it can be seen that, the ZMP constraint, unilateral constraint, and friction constraint are all satisfied.

Second, we give a simulation with initial condition $q(0) = q_s$, $\dot{\theta}(0) = 30^\circ/s$ and $\frac{\partial h_d}{\partial \theta}\big|_{\theta=0} = 0$. From the analysis at the beginning of this subsection, we know the double stance posture designed will be achieved. Figure 6 shows the resulting motion.

The simulated responses of θ with the initial condition $\dot{\theta}(0) = 29^\circ/s$ and $\dot{\theta}(0) = 30^\circ/s$ are shown in Fig. 7. Different values of perturbation result in different final postures. The way of anti-perturbation is very similar to that a human.

https://doi.org/10.1017/S0263574714002215 Published online by Cambridge University Press

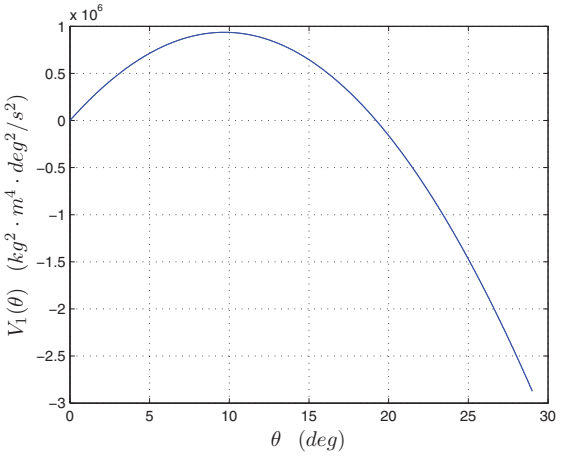


Fig. 3. The value of $V_1(\theta)$ when θ varies from 0° to $\theta_m = 29.0167^\circ$.

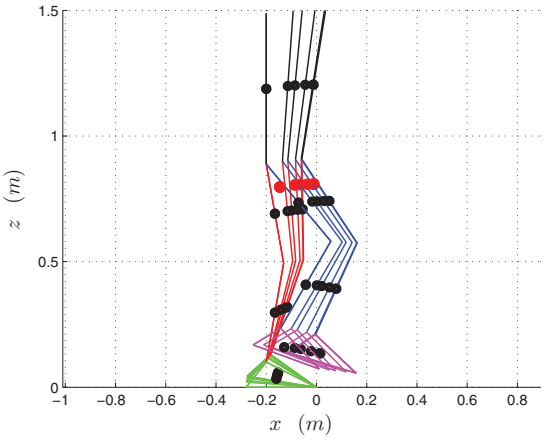


Fig. 4. Stick diagrams of standing with perturbation. The initial condition $\theta(0)$ is 0° and $\dot{\theta}(0)$ is $29^\circ/s$. (The stance leg is red, the swing leg is blue, the torso is black, the stance foot is green, and the swing foot is magenta.).

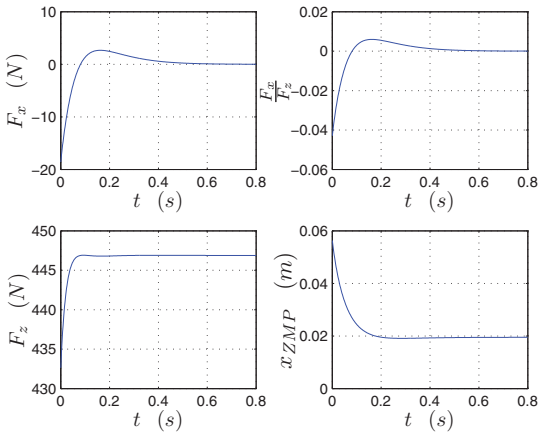


Fig. 5. The simulated responses of the ground reaction force F_x, F_z(N), $\frac{F_x}{F_z}$, and the position of ZMP x_{ZMP}(m) after the impact. The initial condition $\theta(0)$ is 0° and $\dot{\theta}(0)$ is $29^\circ/s$.

https://doi.org/10.1017/S0263574714002215 Published online by Cambridge University Press

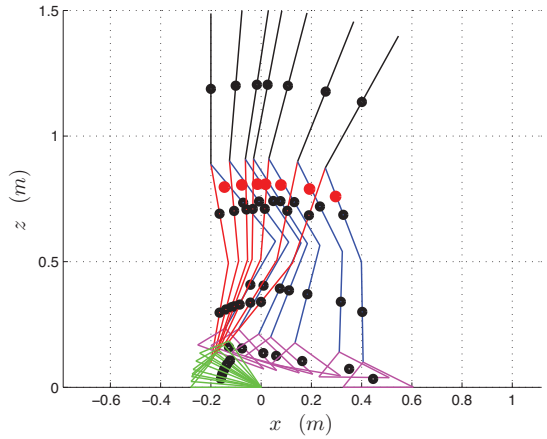


Fig. 6. Stick diagrams of balance control of standing with disturbance. The initial condition $\theta(0)$ is 0° and $\dot{\theta}(0)$ is $30^\circ/s$.

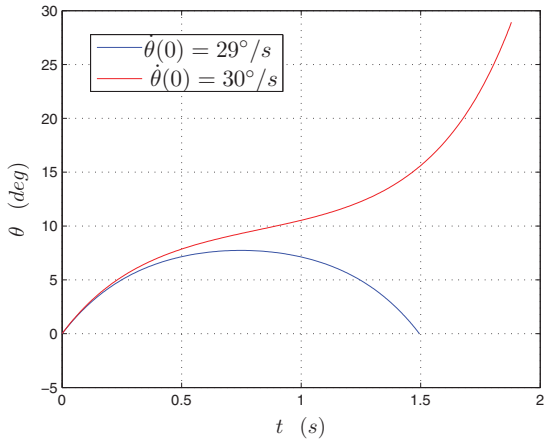


Fig. 7. The simulated responses of θ with the initial condition $\dot{\theta}(0) = 29^\circ/s$ and $\dot{\theta}(0) = 30^\circ/s$, respectively.

5.2. Simulation for toe standing

In this subsection, we design the virtual holonomic constraints so as to make the robot stand on a toe. Also, using *Bézier* polynomials of degree 6, we design the virtual holonomic constraints $h_d(\theta)$ by the optimization method with nonlinear constraints. By Theorem 4.3, we choose $\theta_1 = 10^\circ, \theta_2 = 20^\circ$. The parameters of the polynomials are selected to satisfy a set of nonlinear constraints and to minimize the cost function

$$\max_{\theta_1 \le \theta \le \theta_2} \frac{\partial h_d}{\partial \theta}.$$

The nonlinear constraints are used to ensure that $\kappa_1 > 0$ and that the function $V_1(\theta), \theta \in [\theta_1, \theta_2]$ has a convex downward shape with the minimum value $V_1(\theta^*)|_{\theta^*=15^\circ}$. The function $V_1(\theta), \theta \in [\theta_1, \theta_2]$ is shown in Fig. 8. The value of κ_1 with respect to θ is shown in Fig. 9 and $\kappa_1 > 0$ for $\theta \in [\theta_1, \theta_2]$ is satisfied. Thus, it follows from Theorem 4.4 that $(15^\circ, 0)$ is an asymptotically stable equilibrium point.

We simulate the response with initial condition $\theta(0) = 10.5^\circ$ and $\dot{\theta}(0) = 5^\circ/s$. From Theorem 4.4, we can check that this initial condition is inside the basin of attraction. The diagrams of the resulting motion are provided in Fig. 10. The simulated position of COM x'_{com}, z'_{com}(m) with the balance control for standing on a toe and the desired position of COM x_d, z_d(m) are shown in Fig. 11. The simulated horizontal position of COM x'_{com} with respect to θ is shown in Fig. 12. In addition, the evolution of θ

https://doi.org/10.1017/S0263574714002215 Published online by Cambridge University Press

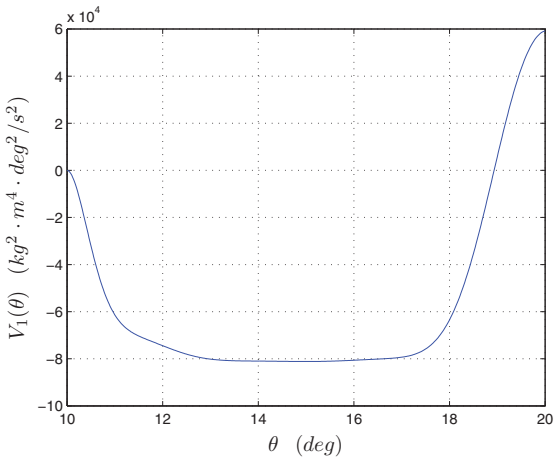


Fig. 8. The value of $V_1(\theta)$ when θ varies from 10° to 20°.

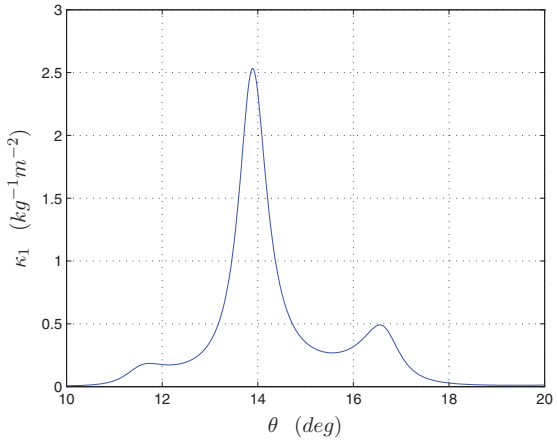


Fig. 9. Plot of θ and κ_1.

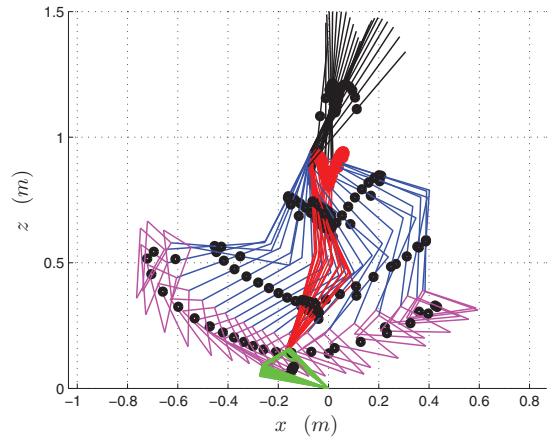


Fig. 10. Stick diagrams of standing on toe. The initial condition $\theta(0) = 10.5°$ and $\dot{\theta}(0) = 5°/s$ and the desired standing angle $\theta^* = 15°$.

is shown in Fig. 13. The evolution trajectory of (σ, θ) in the contour map of V_L is shown in Fig. 14. The trajectory asymptotically converges to the stable equilibrium point $(15°, 0)$, where V_L achieves the minimum value.

https://doi.org/10.1017/S0263574714002215 Published online by Cambridge University Press

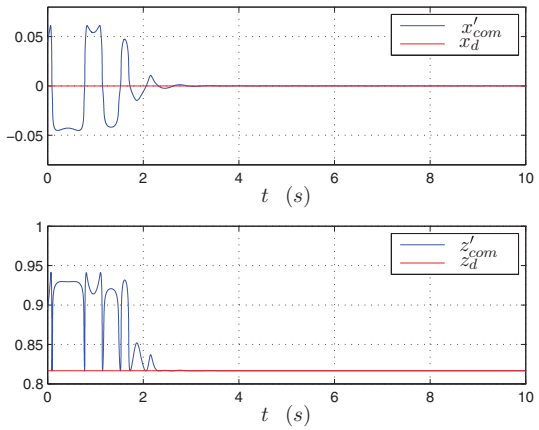


Fig. 11. The simulated position of COM x'_{com}, z'_{com}(m) with the balance control for standing on toe and the desired position of COM x_d, z_d(m).

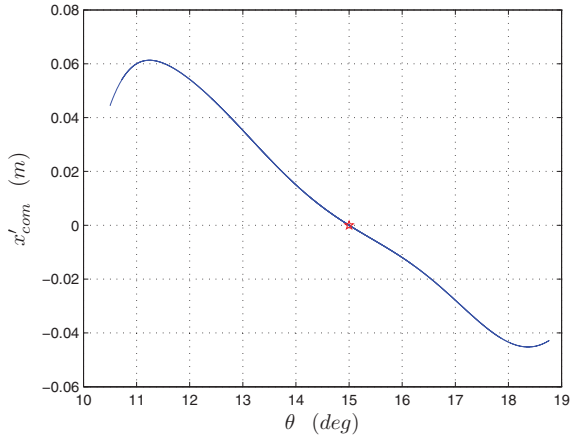


Fig. 12. The simulated horizontal position x'_{com}(m) of COM with respect to θ(deg).

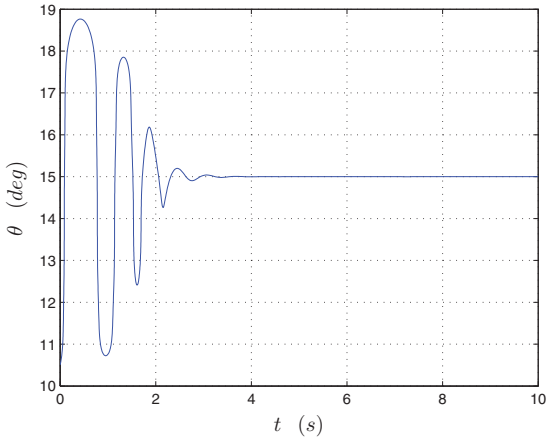


Fig. 13. The simulated response of θ with the initial condition $\theta(0) = 10.5^\circ$ and $\dot{\theta}(0) = 5^\circ/s$.

6. Conclusion

This paper investigates balance control in standing for planar biped robots under disturbances. Human-like foot rotation is a natural response for balance control, which is used as an effective strategy on the biped robots. Furthermore, for a large disturbance leading to a large foot rotation angle, the double stance posture is then applied. This is performed by the pre-designed virtual holonomic constraints.

https://doi.org/10.1017/S0263574714002215 Published online by Cambridge University Press

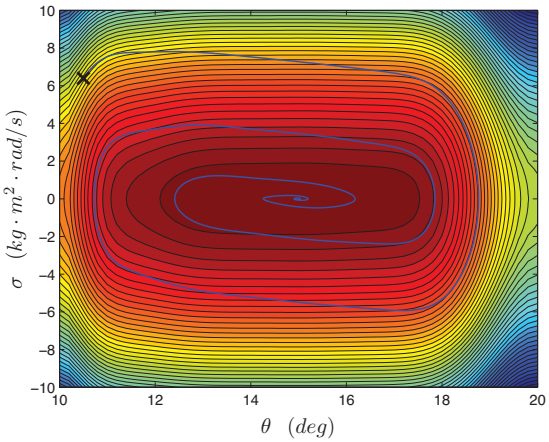


Fig. 14. Evolution of the states in contour map of V_L. The cross is initial point and the blue line is phase trajectory.

We present some analytical conditions for avoiding turnover, which are easy to check. Using this method, standing on a toe is also realized though the robot is underactuated in this situation. A shortcoming of our approach is that the virtual holonomic constraints should be guaranteed and the perturbation only influences the zero dynamics. The test of our results on practical biped robots is considered to be a future work.

Acknowledgments

The work was supported in part by the Key Basic Research and Development Program under Grant 2013CB733100, the National Natural Science Foundation of China under Grant 61333008 and 61304027.

References

1. M. Vukobratovic and B. Borovac, "Zero-moment point–thirty five years of its life," *Int. J. Humanoid Robot.* **1**(1), 157–173 (2004).
2. R. Hirose and T. Takenaka, "Development of the humanoid robot asimo," *Honda R&D Tech. Rev.* **13**(1), 1–6 (2001).
3. T. Ishida, "Development of a Small Biped Entertainment Robot Qrio," *Proceedings of the 2004 International Symposium on Micro-NanoMechatronics and Human Science*, Nagoya, Japan (2004) pp. 23–28.
4. K. Kaneko, F. Kanehiro, S. Kajita, H. Hirukawa, T. Kawasaki, M. Hirata, K. Akachi, and T. Isozumi, "Humanoid Robot hrp-2," *Proceedings of 2004 IEEE International Conference on Robotics and Automation*, New Orleans, USA (2004) pp. 1083–1090.
5. Wikipedia, Humanoid robot. http://en.wikipedia.org/wiki/Humanoid_robot (Apr. 2009).
6. T. Sugihara, Standing Stabilizability and Stepping Maneuver in Planar Bipedalism Based on the Best com-zmp Regulator. *Proceedings of 2009 IEEE International Conference on Robotics and Automation*, Kobe, Japan (2009) pp. 1966–1971.
7. C. Chevallereau, D. Djoudi and J. W. Grizzle, "Stable bipedal walking with foot rotation through direct regulation of the zero moment point," *IEEE Trans. Robot.* **24**(2), 390–401 (2008).
8. D. Goswami and P. Vadakkepat, "Planar bipedal jumping gaits with stable landing," *IEEE Trans. Robot.* **25**(5), 1030–1046 (2009).
9. D. Tlalolini, C. Chevallereau and Y. Aoustin, "Human-like walking: Optimal motion of a bipedal robot with toe-rotation motion," *IEEE/ASME Trans. Mechatronics* **16**(2), 310–320 (2011).
10. R. Ozawa and J. Ishizaki, "Passivity-based Balance Control for a Biped Robot," *Proceedings of 2011 IEEE International Conference on Robotics and Automation, Shanghai, China* (2011) pp. 550–556.
11. A. Shiriaev and J. W. Perram, "Constructive tool for orbital stabilization of underactuated nonlinear systems: Virtual constraints approach," *IEEE Trans. Autom. Control* **50**(8), 1164–1176 (2005).
12. L. Freidovich, A. Robertsson, A. Shiriaev and R. Johansson, "Periodic motions of the pendubot via virtual holonomic constraints: Theory and experiments," *Automatica* **44**(3), 785–791 (2008).
13. L. Consolini and M. Maggiore, "Control of a bicycle using virtual holonomic constraints," *Automatica* **49**(9), 2831–2839 (2013).

https://doi.org/10.1017/S0263574714002215 Published online by Cambridge University Press

14. J. W. Grizzle, G. Abba and F. Plestan, "Asymptotically stable walking for biped robots: analysis via systems with impulse effects," *IEEE Trans. Autom. Control* **46**(1), 51–64 (2001).
15. C. Canudas de Wit, "On the concept of virtual constraints as a tool for walking robot control and balancing," *Annu. Rev. Control* **28**(2), 157–166 (2004).
16. M. Sobotka M. Scheint and M. Buss, "Virtual Holonomic Constraint Approach for Planar Bipedal Walking Robots Extended to Double Support," *Proceedings of 48th IEEE Conference on Decision and Control and 28th Chinese Control Conference*, Shanghai, China (2009) pp. 8180–8185.
17. E. R. Westervelt, J. W. Grizzle, C. Chevallereau, J. H. Choi and B. Morris, *Feedback Control of Dynamic Bipedal Robot Locomotion* (CRC Press, Boca Raton, FL, USA, 2007).
18. D. F. Rogers and J. A. Adams, *Mathematical Elements for Computer Graphics* (McGraw-Hill, New York, USA, 1990).
19. B. Morris and J. W. Grizzle, "Hybrid invariant manifolds in systems with impulse effects with application to periodic locomotion in bipedal robots," *IEEE Trans. Autom. Control* **54**(8), 1751–1764 (2009).
20. A. S. Shiriaev, L. B. Freidovich and I. R. Manchester, "Can we make a robot ballerina perform a pirouette? Orbital stabilization of periodic motions of underactuated mechanical systems," *Annu. Rev. Control* **32**(2), 200–211 (2008).

https://doi.org/10.1017/S0263574714002215 Published online by Cambridge University Press